ResearchGate

See discussions, stats, and author profiles for this publication at: http://www.researchgate.net/publication/260331264

Fabrication and analytical evaluation of three-dimensional microsolenoids achieved in fused silica by femtosecond-laser-based microsolidifying process

ARTICLE *in* MICRO & NANO LETTERS · OCTOBER 2013

Impact Factor: 0.85 · DOI: 10.1049/mnl.2013.0306

READS

36

9 AUTHORS, INCLUDING:

Newkin Liu
Xi'an Jiaotong University
13 PUBLICATIONS **34** CITATIONS

SEE PROFILE

Yang Qing
Xi'an Jiaotong University
75 PUBLICATIONS **418** CITATIONS

SEE PROFILE

Feng Chen
Xi'an Jiaotong University
142 PUBLICATIONS **722** CITATIONS

SEE PROFILE

Guangqing Du
Xi'an Jiaotong University (China)
49 PUBLICATIONS **211** CITATIONS

SEE PROFILE

All in-text references underlined in blue are linked to publications on ResearchGate, letting you access and read them immediately.

Available from: Feng Chen
Retrieved on: 04 November 2015

Fabrication and analytical evaluation of three-dimensional microsolenoids achieved in fused silica by femtosecond-laser-based microsolidifying process

Keyin Liu, Qing Yang, Yulong Zhao, Feng Chen, Chao Shan, Xiaole Fan, Xiangwei Meng, Guangqing Du, Hao Bian

State Key Laboratory for Manufacturing System Engineering and Key Laboratory of Photonics Technology for Information of Shaanxi Province, Xi'an Jiaotong University, Xi'an710049, People's Republic of China
E-mail: chenfeng@mail.xjtu.edu.cn

Published in Micro & Nano Letters; Received on 15th May 2013; Revised on 11th July 2013; Accepted on 17th July 2013

In this reported work, a femtosecond-laser-based microsolidifying method was employed to fabricate three-dimensional (3D) microsolenoids by injecting liquid metal into helicalmicrochannels in fused silica and solidifying the liquid metal, and a proposed finite element method-3D-vector simulation approach was used to analyse the structure influence. An improved femtosecond laser irradiation followed by chemical etching technology was used to fabricate the complex 3D microchannels, in which an optimal laser power compensation strategy of tuning laser power from 7 to 12 mW was involved. Asilanisation process was carried out before the injection process to facilitate the injection of gallium. 3D numerical simulations of the microsolenoids were carried out by an electromagnetic-coupled analysis method; and a simulation-based co-energy calculation method was used to evaluate the inductance of the 3D microsolenoids. 3D microsolenoids of optimised configurations were then achieved according to the analytical results.

1. Introduction: Three-dimensional (3D) microsolenoids have always been critical for miniaturisation of large-scale functional systems, including integrated circuits (ICs), microfluidic systems and microelectromechanical systems (MEMS) [1–5]. Although many efforts have been directed towards 3D microfabrication, it is still a technical challenge to achieve complex 3D microsolenoids[4–7]. The reported microsolenoids were mainly based on the lithographic process which can only provide planar microcoils or microsolenoids of a multiplayer structure, not to mention the tedious fabricating process and expensive cost.

At the same time, analytical evaluation of microsolenoids has mostly concentrated on the 2D planar spirals. Nowadays, the performance prediction of 3D microsolenoids mainly depends on the empirical formula or scalar analysis by the finite element method (FEM) [8–12]. These methods have limitations to the precise calculation or prediction of the properties of microscale solenoids owing to their lack of considering the unique geometry configurations of 3D microsolenoids, such as a greater ratio of helix pitch to radius etc. However, the reported 3D microsolenoids, which have been applied in on-chip nuclear magnetic resonance (NMR) and other microsystems [1–5], mostly consist of a sparse structure with a large ratio of helix pitch to coil radius; and the influence of the wire diameter cannot be neglected.

With the development of femtosecond laser technology, a femtosecond laser irradiation followed by chemical etching (FLICE) technology has been utilised to fabricate complex 3D microchannels in fused silica [13–16]. In this Letter, a femtosecond-laser-based microsolidifying process is proposed to fabricate 3D cylindrical microsolenoids by combining the FLICE technology and liquid-metal-injection technology. Meanwhile, 3D microsolenoids of different geometrical parameters were modelled and numerically simulated using a FEM-3D-vector analysis method. The simulation process involves 3D electricmagnetic-coupled FEM calculation using ANSYS software which can more precisely calculate the properties of 3D microsolenoids. A simulation-based co-energy calculation method was subsequently used to evaluate the inductance of the 3D microsolenoids. Lastly, microsolenoids of optimised configurations were fabricated according to the simulation results. Typically, this simulation method is beneficial for the optimal design and performance prediction of 3D microsolenoids.

2. Methods development

2.1. Structure design and fabrication: Cylindrical coils have proven to be the most efficient structure as solenoids than other structures. Although cylindrical air-core solenoids have lower inductance than ferromagnetic core coils, yet they are often used at high frequencies because they are free from energy losses called core losses that occur in ferromagnetic cores, which increase with frequency. Moreover, the cylindrical air-core coils have been defined as key elements in microfluidic applications, especially in the NMR microsystems [5].

3D helical microchannels in fused silica, which served as the micromoulds of the 3D solenoids, were fabricated by selective etching of fused silica after femtosecond laser irradiation, as shown in Fig. 1*a*. The femtosecond laser micromachining system consists of a femtosecond laser source (wavelength: 800 nm, pulse duration: 50 femtosecond, repetition rate: 1 kHz), a microscope objective, a programmable three-axis stage, a CCD camera and a laser beam control system. During the laser irradiation process, the bulk fused silica ($10 \times 10 \times 0.8\ mm^3$) was fixed on the three-axis stage; and the designed patterns were written in fused silica with femtosecond laser pulses by translating the bulk fused silica along the programmed pattern path. The chemical etching process was carried out in hydrofluoric (HF) acid solution assisted by the ultrasonic bath. The processing parameters were kept constant as: scanning speed of 10 $\mu m\ s^{-1}$ and HF solution concentration of 10%. A circular-polarisation laser was used to eliminate the polarisation influence on etching efficiency [16] because the circular-polarisation laser contributes to isotropous modification of the irradiated region, and the velocity direction of the laser beam scanning complex 3D patterns is changing in 3D. Then, liquid metal of gallium (Ga, mp $\simeq 30^\circ C$) was injected into the microchannels and solidified to form the microsolenoids. In addition, a silanisation process was carried out before the injection of gallium to decrease the free energy of the metal–silica interface of the channels.

2.2. Analytical evaluation: 3D microsolenoids of different geometrical parameters were modelled and numerically simulated using a FEM-3D-vector analysis method rather than traditional FEM-scalar analysis. The simulation process involves the FEM

© The Institution of Engineering and Technology 2013

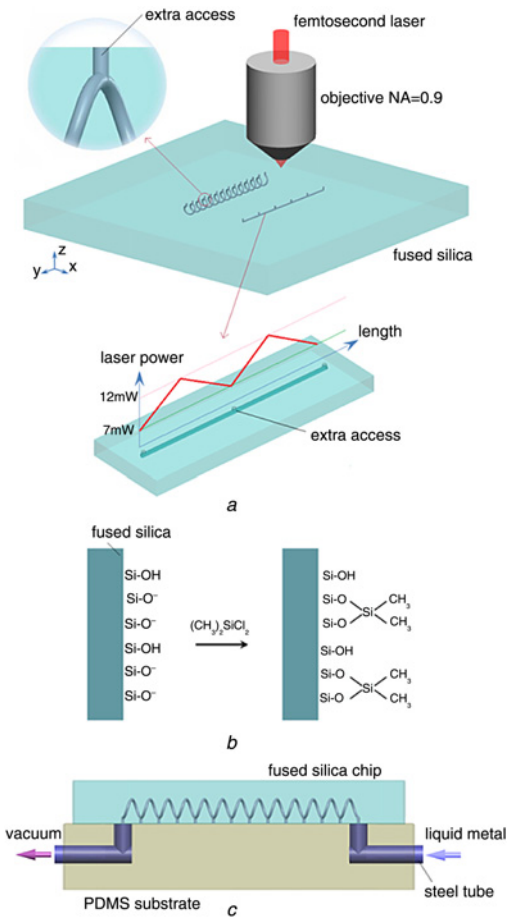

Figure 1 *Schematic illustration of the femtosecond-laser-based microsolidifying process*
a Improved FLICE technology of writing complex 3D microstructures with extra accesses and laser power compensation
b Silanisation process of the inner surface of the microchannels
c Illustration of the microsolidifying process and the microfluidic-compatible injection device

3D electricmagnetic-coupled calculation using ANSYS software. A direct current of 0.2 A was applied on the 3D microsolenoids in the simulation process, and the magnetic field or magnetic flux density was then simulated. A simulation-based co-energy calculation method was used to evaluate the inductance of the 3D microsolenoids, according to the formula

$$W_L = \frac{1}{2} L I^2 \tag{1}$$

where W_L is the stored magnetic co-energy of the 3D microsolenoids, L is the inductance and I is the current through the inductor.

This simulation process has taken into consideration the number of coils N, the solenoid length L, the solenoid diameter D, the wire diameter d and the helical pitch H; and it can more precisely predict the 3D microsolenoid performance. As shown in Fig. 2, the simulation results of a straight microsolenoid were demonstrated with geometrical parameters: $N = 20$, $H = 125$ µm, $D = 200$ µm and $d = 30$ µm; the solenoid length is determined by the number of coils and helical pitch as 2.5 mm.

3. Results and discussion

3.1. Realisation of 3D microsolenoids: The reported studies have demonstrated that the selective etching of fused silica after laser irradiation is associated with the femtosecond-laser-induced micro/nanocracks in the material [17] or modification of the substance [18]. The microchannels of millimetres fabricated by the traditional FLICE technology are usually strongly tapered when a conical geometry in the microchannel is unavoidable, and the FLICE technology is generally used to provide microchannels in fused silica of less than a few millimetres [15, 16]. Based on our previous work [19, 20], methods of fabricating complex 3D microstructures with extra accesses and laser power compensation were employed to improve the processing capability as shown in Fig. 1*a*.

The extra accesses acted as extra entrances for the etching solution during the etching process. The amount and distribution of the extra access was designed according to the geometry of the microchannels. According to our previous study [19], the diameter of the microchannels is increased with laser power from 1 to 27 mW. However, the microchannels fabricated with a high power (>15 mW) are accompanied with cracks and a rough inner surface which will be disadvantages for the injection of liquid metal. At the same time, the laser with a low power (< 5 mW) cannot induce an efficient modification effect for the irradiated region of fused silica, and microchannels with a great depth and large scale cannot be achieved. Accordingly, the optimal fabricating strategy of tuning laser power during the laser irradiation process was used to improve the microchannel geometry quality. In the experiment, the laser power was modified linearly from 7 mW at the entrances/extra access to 12 mW in the middle of two adjacent entrances by a computer-controlled attenuator to compensate for the conical geometry in the microchannel.

For microchannels with a diameter >35 µm, liquid gallium can easily fill the microfluidic channels completely; non-uniform wetting of the microfluidic channels was rarely observed. However, liquid gallium in narrower microchannels (diameter <30 µm) was often accompanied with non-uniform wetting points, and sometimes the liquid gallium in the microchannels was separated as disconnected parts. As the diameter of the microchannels decreased to 20 µm, it became difficult to pull the liquid gallium through the microfluidic channels. This phenomenon was caused by the poor microscale wetting characteristics of liquid gallium with fused silica. To improve the wetting characteristics and fabricate more miniaturised metallic devices, silanisation of microcavities before the injection of gallium was carried out using dimethylchlorosilane, as described in Fig. 1*b*. After this process, the inside surface of the channels was coated with a layer of silane; and the silane decreased the free energy of the metal–silica interface of the channels and made it possible to wet the inside walls with liquid gallium. This process enabled efficient fabrication of metallic structures in microchannels with a narrower diameter (20–30 µm).

Fig. 3 shows the fabricated 3D microchannels and metallic microsolenoids. Fig. 3*d* shows a microfluidic system consisting of a straight microcoil and a central microchannel along the axis of the microcoil; and deionised water, which can be replaced by biochemical solutions, was easily introduced into the microfluidic system.

3.2. Comparison and analysis: For short cylindrical air-core coils, one can use the well-known Nagaoka formula [8] to calculate the inductance L

$$L = \frac{K \mu_0 N^2 \pi D^2}{4\,L} \tag{2}$$

where N is the coil number of solenoid, D is the solenoid diameter, L is the length of the solenoid and K is the shape factor related to the ratio of solenoid diameter to solenoid length (D/L). The Nagaoka formula has the inconvenience of requiring a list of tabulated values for different diameter/length ratios. Another formula,

© The Institution of Engineering and Technology 2013

doi: 10.1049/mnl.2013.0306

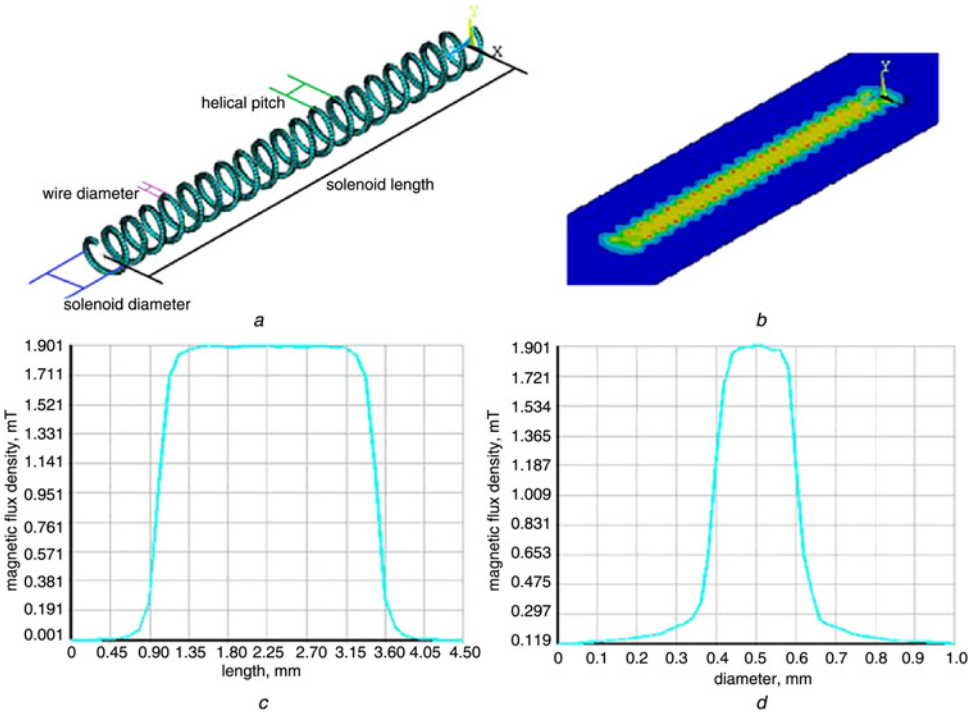

Figure 2 *Simulation results of a 3D microsolenoid*
a Structural schematic diagram
b Magnetic flux density distribution on the solenoid diameter–length section
c Magnetic flux density along the central axis
d Magnetic flux density along the solenoid diameter at the end face

Wheeler's formula [9], can also be used to calculate the inductance of short coils, which is the asymptotic approximation of the Nagaoka formula.

Comparison of the Nagaoka formula and the FEM-3D-vector analysis was carried out to calculate the inductance: varying one of the four geometrical parameters (the coil number of solenoid

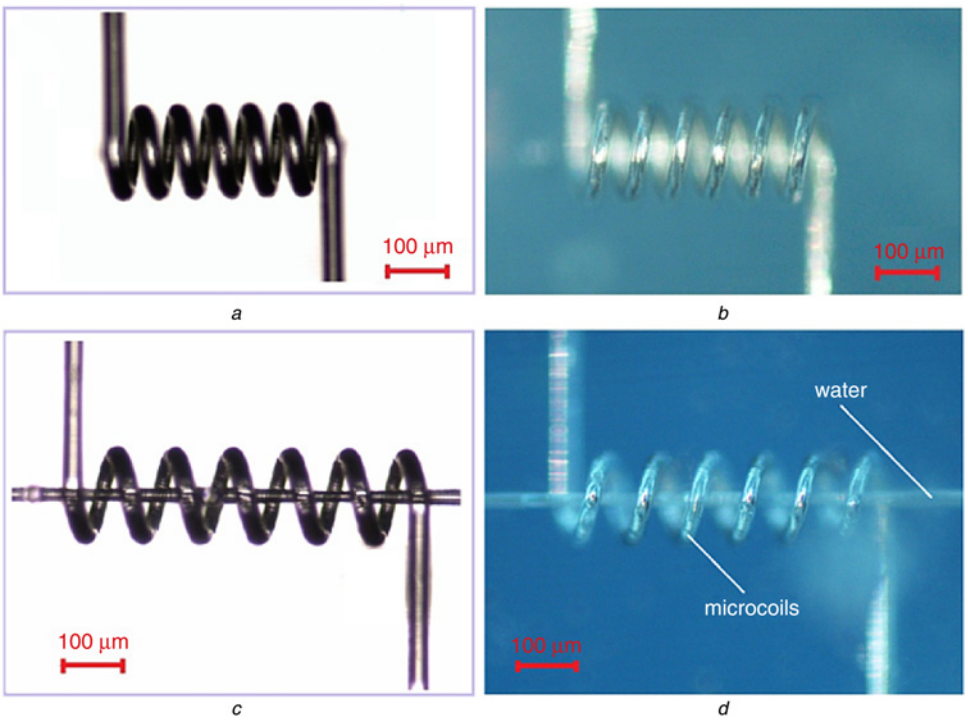

Figure 3 *3D helical microchannels and microsolenoids fabricated by the femtosecond-laser-based microsolidifying process*
a 3D Helical microchannel
b 3D Microcoil
c 3D Helical microchannel with central channel
d 3D Microcoil with central microchannel filled with water

© The Institution of Engineering and Technology 2013

N, the solenoid diameter D, the length of the solenoid L and the wire diameter d) while keeping the other three geometrical parameters constant. A relative error was employed to evaluate the calculation accuracy of the Nagaoka formula:

$$\text{Relative error} = \frac{|\text{Simulation result} - \text{Calculation result}|}{\text{Simulation result}} \times 100\% \quad (3)$$

Fig. 4 shows the simulation and comparison results: (Fig. 4*a*) varying solenoid diameter 80–360 µm, keeping number of coils as 10, wire diameter 10 µm and solenoid length 1 mm; (Fig. 4*b*) varying solenoid length 0.2–2.5 mm, keeping number of coils as 10, wire diameter 10 µm and solenoid diameter 200 µm; (Fig. 4*c*) varying number of coils 2–23, keeping solenoid length as 1 mm, wire diameter 10 µm and solenoid diameter 200 µm; (Fig. 4*d*) relationship of the relative error and the ratio of helical pitch to solenoid diameter (*H*/*D*); and (Fig. 4*e*) relationship of the solenoid inductance and the ratio of wire diameter to solenoid diameter (*d*/*D*): varying wire diameter 5–80 µm, keeping solenoid diameter as 200 µm, number of coils 10 and solenoid length 1 mm.The results show that the relative error increases with the ratio of helical pitch to solenoid diameter (*H*/*D*). Although the results of the simulation and the calculation coincide with each other well at little *H*/*D*, the Nagaoka formula is not suitable for sparse solenoids with large *H*/*D*.

As shown in Fig. 4*d*, the relative errors of varying solenoid length and varying the number of coils are consistent with each other; the relative error of varying solenoid diameter is less than the other two. It means the simulation–calculation difference of varying solenoid diameter is less than that of varying solenoid length or varying the number of coils. The difference of the three simulation processes exists in the geometrical influence of the wire diameter: the ratio of wire diameter to solenoid diameter (*d*/*D*) changes while varying solenoid diameter. The simulation results indicate that the inductance decreases while increasing *d*/*D*, as shown in Fig. 4*e*. The ratio of *d*/*D* (0.028–0.25) increases with *H*/*D* (0.28–1.25) in the simulation process of varying solenoid diameter, however it remains constant in the other two simulation processes. Thus, the incensement of *d*/*D* with *H*/*D* contributes to the decrease of solenoid inductance and the simulation–calculation difference.

The Nagaoka formula nor the Wheeler's formula do not take into account wire diameter and spacing between the turns, which means

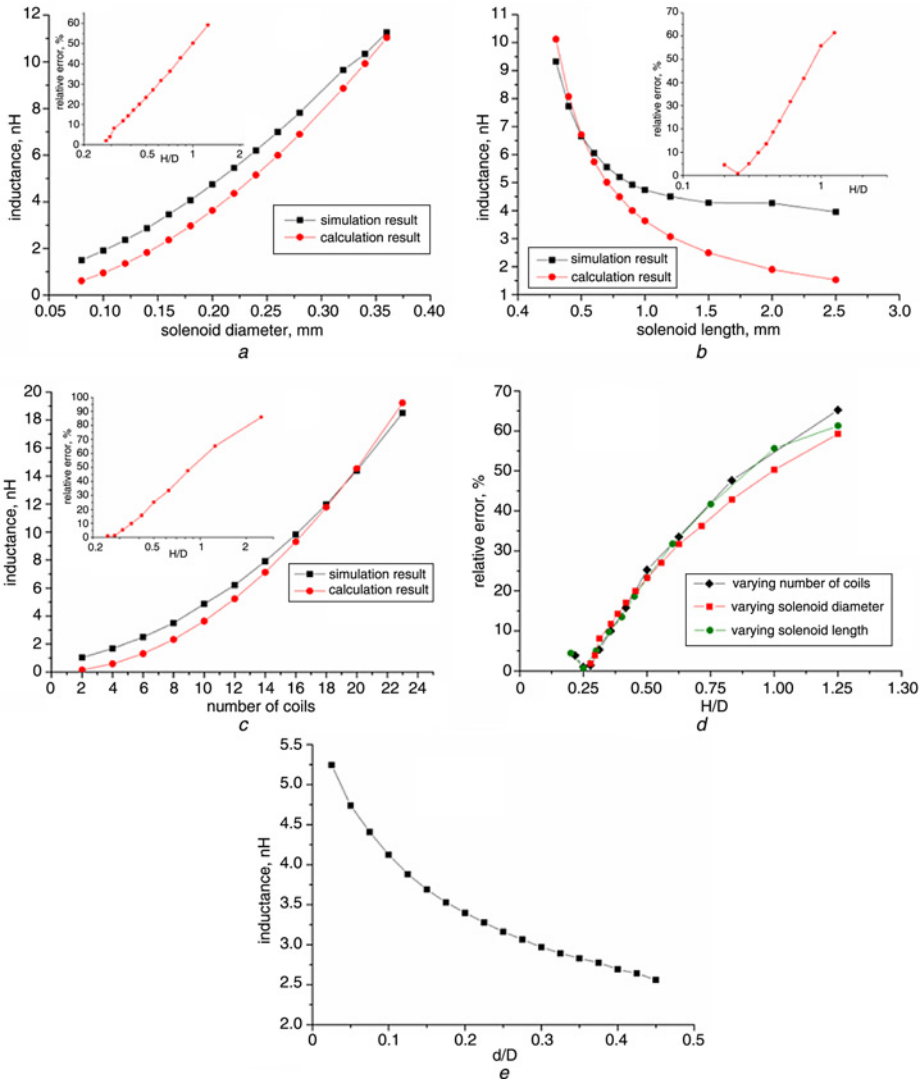

Figure 4 *Simulation results of the FEM-3D-vector analysis and Nagaoka formula calculation*
a Varying solenoid diameter
b Varying solenoid length
c Varying number of coils
d Relationship of the relative error and the ratio of helical pitch to solenoid diameter (*H*/*D*)
e Relationship of the solenoid inductance and the ratio of wire diameter to solenoid diameter (*d*/*D*)

© The Institution of Engineering and Technology 2013

doi: 10.1049/mnl.2013.0306

they are based on densely-winded uniform straight solenoids. The turns are touching each other in these formulae, but some insulation is assumed to prevent shorting in practice. Actually, some kind of large spacing between turns is unavoidable in most reported microsolenoids; the reported microcoils mostly consist of a sparse structure applied in microfluidic systems, on-chip NMR systems etc. The FEM-3D-vector analysis concentrates more on the microsolenoids' geometry and is almost completely approaching the real 3D microsolenoids. Thus, the FEM-3D-vector analysis is more suitable for the microsolenoids whose performance is largely determined by their typical geometrical construction.

3.3. Construction extension: Another advantage of the FEM-3D-vector analysis method is the convenience to evaluate more complex 3D microsolenoids other than straight ones. As shown in Fig. 5, 3D microsolenoids of U shape and O shape were modelled and simulated by the FEM-3D-vector analysis method; the magnetic flux density distribution on the solenoid diameter–length section and magnetic flux density along the circle diameter (along the red lines in Fig. 5) were characterised, respectively. The geometrical parameters were kept the same as the straight microsolenoid shown in Fig. 2 as: $N = 20$, $H = 125\ \mu m$, $D = 200\ \mu m$, $d = 30\ \mu m$ and centreline diameter 800 µm. The simulated solenoid inductances were 7.04 nH for the straight microsolenoid, 6.897 nH for the U-shape microsolenoid and 7.345 nH for the O-shape microsolenoid. The O-shape microsolenoid has the biggest solenoid inductance, because it is accompanied with the minimum magnetic flux leakage with a circular structure.

The femtosecond-laser-based microsolidifying technology has a flexible processing capability of 3D microsolenoids; and 3D microsolenoids of intricate constructions according to the optimal design can be achieved. Fig. 6 shows the fabricated 3D U-shape and O-shape microsolenoids with the geometrical parameters the same as the simulation structures in Fig. 5.

The femtosecond-laser-based microsolidifying method also has some limitations. The improved femtosecond laser irradiation followed by chemical etching (FLICE) technology involved in the fabricating process is accompanied with an extra access structure which may have side effects on microsolenoid performance.

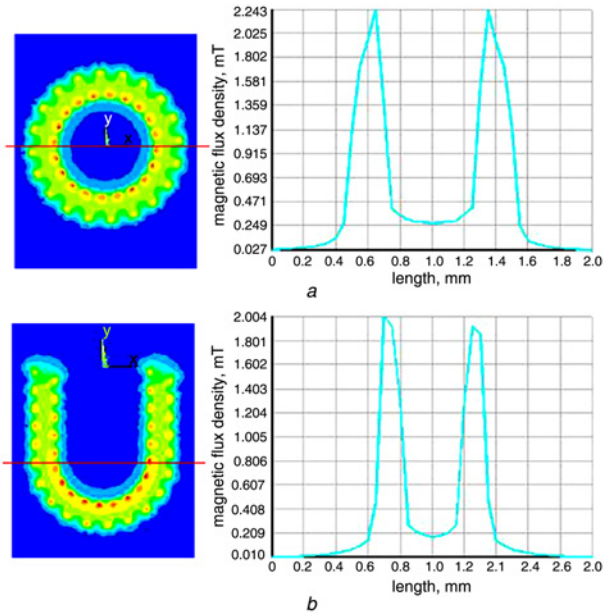

Figure 5 *Simulation results of 3D microsolenoids*
a O-shape
b U-shape

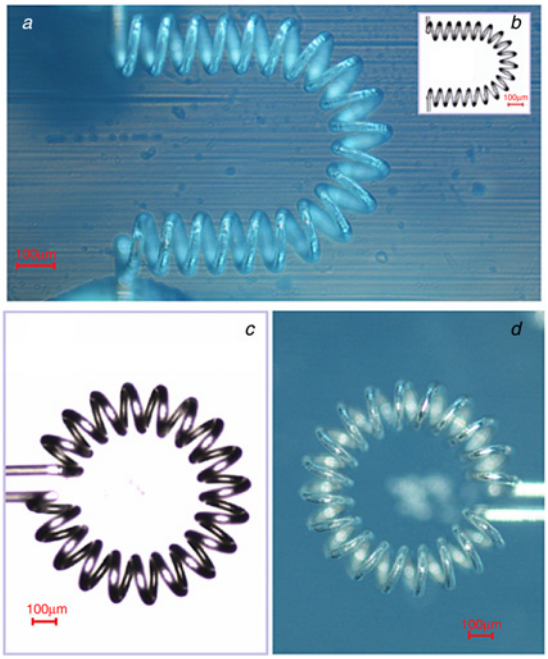

Figure 6 *3D microsolenoids of U-shape and O-shape fabricated by the femtosecond-laser-based microsolidifying process*
a, *b* U-shape helical microchannels and microsolenoids
c, *d* O-shape helical microchannels and microsolenoids

However, the side effects of the extra access structure could be eliminated or decreased by decreasing the length of extra access or filling the extra access with polymeric materials. In addition, the low-melting point of gallium may not meet a wide range of operation temperatures; but as a vast kind of reported low-melting point metals [7] can be used to form the 3D microsolenoids, the femtosecond-laser-based microsolidifying method will be beneficial for the fabrication of microsystems, for example, microfluidic systems. Meanwhile, the FEM-3D-vector analysis is a static analysis process. It needs further analysis to study the microsolenoid performance at high frequencies, such as the influence of skin effect where the current density is largest near the surface of the solenoid. However, this facile analysis method can provide more precise static evaluation of the 3D microsolenoid with a sparse structure, and is beneficial for optimal design.

4. Conclusion: This Letter presents a femtosecond-laser-based microsolidifying technique to fabricate intricate 3D microsolenoids in fused silica, and a FEM-3D-vector simulation approach was proposed to analyse the structure's influence. The femtosecond-laser-based microsolidifying technique method has several advantages over other techniques to fabricate 3D microsolenoids: the fabricating procedure is facile and maskless, and makes it possible to fabricate 3D microsolenoids with arbitrary configuration. 3D numerical simulations of the microsolenoids are carried out by a FEM-3D-vector analysis method; and a simulation-based co-energy calculation method was used to evaluate the inductance of the 3D microsolenoids. More accurate prediction results can be gained than with the empirical formula. The fabricating and analysing methods in this study will be beneficial for the application of complex 3D microsolenoids.

5. Acknowledgments: This work is supported by the National Natural Science Foundation of China under grant no. 61176113, the Program for Changjiang Scholars and Innovative Research Team in University (IRT1033) and the Fundamental Research Funds for the Central Universities of China.

© The Institution of Engineering and Technology 2013

6 References

[1] Gao X.Y., Zhou Y., Cao Y., *ET AL.*: 'A copper/polyimide fabrication process for fabricating high-inductance microinductor', *IEEE Trans. Electron. Packag. Manuf.*, 2007, **30**, pp. 123–127

[2] Ding L.Y., Shih W.P., Hu Y.C., Chen Y.J., Chang P.Z.: 'CMOS compatible electrochemical process for improving quality factor of spiral microinductors', *Micro Nano Lett.*, 2010, **5**, pp. 266–269

[3] Badilita V., Kratt K., Baxan N., *ET AL.*: 'On-chip three dimensional microcoils for MRI at the microscale', *Lab. Chip*, 2010, **10**, pp. 1387–1390

[4] Cao Y.Y., Takeyasu N., Tanaka T., Duan X.M., Kawata S.: '3D metallic nanostructure fabrication by surfactant-assisted multiphoton-induced reduction', *Small*, 2009, **5**, pp. 1144–1148

[5] Kong T.F., Peng W.K., Luong T.D., Nguyen N.T., Han J.: 'Adhesive-based liquid metal radio-frequency microcoil for magnetic resonance relaxometry measurement', *Lab. Chip*, 2012, **12**, pp. 287–294

[6] Bae K.M., Ko J.S., Lim T.W., *ET AL.*: 'Direct reproduction of 3D microstructures using a hybrid approach: by creation of master-patterns and metallic molds for embossing', *Microelectron. Eng.*, 2011, **88**, pp. 3300–3305

[7] Siegel A.C., Bruzewicz D.A., Weibel D.B., Whitesides G.M.: 'Microsolidics: fabrication of three-dimensional metallic microstructures in poly (dimethylsiloxane)', *Adv. Mater.*, 2007, **19**, pp. 727–733

[8] Nagaoka H.: 'The inductance coefficients of solenoids', *J. Coll. Sci.*, 1909, **27**, pp. 18–33

[9] Wheeler H.A.: 'Inductance formulas for circular and square coils', *Proc. IEEE*, 1982, **70**, pp. 1449–1450

[10] Santra A., Chakraborty N., Ganguly R.: 'Analytical evaluation of magnetic field by planar micro-electromagnet spirals for MEMS applications', *J. Micromech. Microeng.*, 2009, **19**, p. 085018

[11] Tsui H.Y., Lau J.: 'An on-chip vertical solenoid inductor design for multigigahertz CMOS RFIC', *IEEE Trans. Microw. Theory Tech.*, 2005, **53**, pp. 1883–1890

[12] Gyimesi M., Ostergaard D.: 'Inductance computation by incremental finite element analysis', *IEEE Trans. Magn.*, 1999, **35**, pp. 1119–1122

[13] Liao Y., Song J., Li E., Luo Y., Shen Y., Chen D.: 'Rapid prototyping of three dimensional microfluidic mixers in glass by femtosecond laser direct writing', *Lab. Chip*, 2012, **12**, pp. 746–749

[14] Malek C.G.K.: 'Laser processing for bio-microfluidics applications (Part II)', *Anal. Bioanal. Chem.*, 2006, **385**, pp. 1362–1396

[15] Maselli V., Osellame R., Cerullo G., Ramponi R., Laporta P.: 'Fabrication of long microchannels with circular cross section using astigmatically shaped femtosecond laser pulses and chemical etching', *Appl. Phys. Lett.*, 2006, **88**, p. 191107

[16] Hnatovsky C., Taylor R.S., Simova E., Bhardwaj V.R., Rayner D.M., Corkum P.B.: 'Polarization-selective etching in femtosecond laser-assisted microfluidic channel fabrication in fused silica', *Opt. Lett.*, 2005, **30**, pp. 1867–1869

[17] Hnatovsky C., Taylor R.S., Simova E., *ET AL.*: 'Fabrication of microchannels in glass using focused femtosecond laser radiation and selective chemical etching', *Appl. Phys. A*, 2006, **84**, pp. 47–61

[18] Andrius M., Saulius J.: 'Femtosecond laser-assisted three-dimensional microfabrication in silica', *Opt. Lett.*, 2001, **26**, pp. 277–279

[19] He S.G., Chen F., Liu K.Y., *ET AL.*: 'Fabrication of three-dimensional helical microchannels with arbitrary length and uniform diameter inside fused silica', *Opt. Lett.*, 2012, **37**, pp. 3825–3827

[20] He S.G., Chen F., Yang Q., *ET AL.*: 'Fabrication of true three-dimensional microcoils inside silica by a femtosecond laser', *J. Micromech. Microeng.*, 2012, **22**, p. 105017

© The Institution of Engineering and Technology 2013

doi: 10.1049/mnl.2013.0306